

**JMB**Available online at [www.sciencedirect.com](http://www.sciencedirect.com) ScienceDirect

# Crystallographic Evidence for Water-assisted Photo-induced Peptide Cleavage in the Stony Coral Fluorescent Protein Kaede

Ikuko Hayashi<sup>1</sup>, Hideaki Mizuno<sup>2</sup>, Kit I. Tong<sup>1</sup>, Toshiaki Furuta<sup>3</sup>  
Fujie Tanaka<sup>4</sup>, Masato Yoshimura<sup>5</sup>, Atsushi Miyawaki<sup>2</sup>  
and Mitsuhiko Ikura<sup>1\*</sup>

<sup>1</sup>Division of Signaling Biology  
Ontario Cancer Institute and  
Department of Medical  
Biophysics, 101 College St.  
Toronto, Ontario, M5G 1L7  
Canada

<sup>2</sup>Laboratory for Cell Function  
and Dynamics, Advanced  
Technology Development  
Group, Brain Science  
Institute, RIKEN, 2-1  
Hirosawa, Wako-city  
Saitama, 351-0198, Japan

<sup>3</sup>Department of Biomolecular  
Science and Research Center  
for Advanced Materials with  
Integrated Properties, Toho  
University, 2-2-1 Miyama  
Funabashi, Chiba  
274-8510, Japan

<sup>4</sup>Department of Molecular  
Biology, The Scripps  
Research Institute, 10550  
North Torrey Pines Road  
La Jolla, CA 92037, USA

<sup>5</sup>Institute for Protein Research  
Osaka University, Yamadaoka  
3-2, Suita, Osaka 565-0871  
Japan

A coral fluorescent protein from *Trachyphyllia geoffroyi*, Kaede, possesses a tripeptide of His62-Tyr63-Gly64, which forms a chromophore with green fluorescence. This chromophore's fluorescence turns red following UV light irradiation. We have previously shown that such photoconversion is achieved by a formal  $\beta$ -elimination reaction, which results in a cleavage of the peptide bond found between the amide nitrogen and the  $\alpha$ -carbon at His62. However, the stereochemical arrangement of the chromophore and the precise structural basis for this reaction mechanism previously remained unknown. Here, we report the crystal structures of the green and red form of Kaede at 1.4 Å and 1.6 Å resolutions, respectively. Our structures depict the cleaved peptide bond in the red form. The chromophore conformations both in the green and red forms are similar, except a well-defined water molecule in the proximity of the His62 imidazole ring in the green form. We propose a molecular mechanism for green-to-red photoconversion, which is assisted by the water molecule.

© 2007 Elsevier Ltd. All rights reserved.

\*Corresponding author

**Keywords:** Kaede; fluorescent protein; crystal structure; photoconversion;  $\beta$ -elimination reaction

Abbreviations used: GFP, green fluorescent protein;  
r.m.s.d., root-mean-square deviation.

E-mail address of the corresponding author:  
[mikura@uhnres.utoronto.ca](mailto:mikura@uhnres.utoronto.ca)

## Introduction

The green fluorescent protein (GFP) from *Aequorea victoria* is the prototype of a family of fluorescent proteins in which visible fluorescence is genetically encoded. GFP has been studied extensively and proven to be an indispensable tool in molecular

biology and biotechnology.<sup>1</sup> Crystallographic and biophysical studies showed GFP as an 11-stranded  $\beta$ -barrel structure with a central  $\alpha$ -helix which contains a fluorescent chromophore.<sup>2</sup> Spontaneous generation of the fluorescent chromophore is achieved by cyclization of Ser65-Tyr66-Gly67 within the central  $\alpha$ -helix.<sup>3</sup> This cyclization and subsequent dehydrogenation of the C $^{\alpha}$ -C $^{\beta}$  bond of Tyr66 result in an extended, conjugated  $\pi$ -system of heterocyclic imidazoline ring. Although the  $\pi$ -resonance system accounts largely for visible absorbance with a maximum wavelength of 475 nm, energetic interactions between the chromophore and the  $\beta$ -barrel structure are crucial to the optical property of GFP.<sup>4</sup> Based on the crystal structure of GFP, a large number of mutants have been engineered to alter absorption and emission spectra by manipulating the  $\pi$ -resonance system and its environment.<sup>3,5</sup> One example is the yellow fluorescent variant of GFP (YFP) with a mutation from Thr to Tyr at the 203rd position.<sup>6</sup> In the crystal structure of YFP, the highly polarized Tyr203 side-chain stacks with the phenolic moiety of the chromophore, leading to a red shift in the fluorescent spectrum. These color mutants of GFP have been used to probe cellular and sub-cellular distributions of multiple target proteins and provided tools for fluorescent resonance energy transfer (FRET) in order to determine intracellular calcium concentration or pH at localized sites, and to follow protein-protein interactions.<sup>7,8</sup> Genetic engineering of GFP thus far, however, has yielded only a limited number of color variants with the longest emission wavelength at 529 nm.<sup>3,9</sup>

The discovery of new fluorescent proteins from the non-bioluminescent *Anthozoa* species, in particular the red-shifted fluorescent protein DsRed expanded the application of fluorescent proteins in multicolor labeling applications.<sup>5,10-12</sup> This new GFP variant protein displays excitation and emission bands at 558 nm and 583 nm, respectively. DsRed is a distant homolog of GFP (23% sequence identity), forming a tetramer in solution. Crystallographic studies of DsRed have shown that the tripeptide Gln66-Tyr67-Gly68 is responsible for chromophore formation. Although the basic  $\pi$ -resonance system of GFP is retained in DsRed, the DsRed-specific spectral properties arise from a unique chromophore environment with some modifications, extending from the coplanar  $\pi$ -resonance system of the chromophore. Other examples are far-red fluorescent proteins, HcRed and eqFP611, that when excited, emit light maximally at 645 nm and 611 nm, respectively.<sup>13,14</sup> HcRed possesses a chromophore of Glu-Tyr-Gly with conformational flexibility,<sup>13</sup> whereas eqFP611 with a Met-Tyr-Gly chromophore adopting a novel coplanar and *trans* conformation.<sup>15</sup>

Recently, the fluorescent proteins called Kaede and EosFP are discovered from a stony coral, *Trachyphyllia geoffroyi* and *Lobophyllia Hemprochii*, respectively, with a tripeptide His62-Tyr63-Gly64, at the chromophore position.<sup>16,17</sup> Irradiation of these proteins by UV/VIS light (350 nm–410 nm)

results in photoconversion from green to red. Our previous NMR and mass spectroscopic analysis of Kaede has provided evidence for the new red-emitting chromophore of 2-[(1E)-2-(4-imidazolyl)ethenyl]-4-(*p*-hydroxybenzylidene)-5-imidazolone, which results from the peptide cleavage at His62 by a formal  $\beta$ -elimination reaction.<sup>18</sup> Peptide cleavage has been reported in several fluorescent proteins such as DsRed, gtCP, zFP538, KFP and EosFP.<sup>17,19-23</sup> The induction of the break is different among the proteins: DsRed and gtCP upon boiling, zFP538 and KFP by autocatalytic process, Kaede and EosFP by UV irradiation. Nienhaus *et al.*<sup>24</sup> recently reported the crystal structure of EosFP in both the green and red forms. This structural study provided first atomic-resolution insight into mechanisms underlying the photo-induced peptide cleavage of fluorescent proteins. However, the proposed mechanism of the photoconversion raised a question in terms of predicted chemical structures of reaction intermediates.

Here we present the crystal structure of Kaede in two forms, one before and one after UV irradiation. High resolution X-ray data provide atomic-level evidence for the proposed photo-induced peptide cleavage required for the red-chromophore formation.<sup>18</sup> Our crystallographic data showed that the chromophore structures of the green and red forms are distinct from each other, but the environments of the chromophores between green and red forms are surprisingly very similar. Based on our crystal structures of the green and red forms, we propose a water-mediated reaction mechanism of the UV/vis irradiation-initiated conversion from the green to red form in Kaede, which differs from the mechanism for EosFP photoconversion proposed by Neunhaus *et al.*<sup>24</sup>

## Results and Discussion

### Overview of the structure

The crystal structures of the green and red forms of Kaede belong to the space group C2 with two non-crystallographic symmetry (NCS) related protomers (chain A and B in Figure 1(a)) per asymmetric unit. Compared to other members of the GFP family whose structures are known at this time, the Kaede primary sequence is most similar to that of EosFP (84% sequence identity; Table 1; Supplementary Data, Figure 1) whose structures were solved recently.<sup>24</sup> The structure of EosFP was not available when we analyzed the structure of Kaede. We used a monomer structure of DsRed (PDB code, 1G7K; 47% sequence similarity), the closest homologue structurally available at the moment, and determined the crystal structures of Kaede both before and after UV irradiation by molecular replacement. The Kaede protomer has a very similar fold to that for GFP or DsRed, pos-

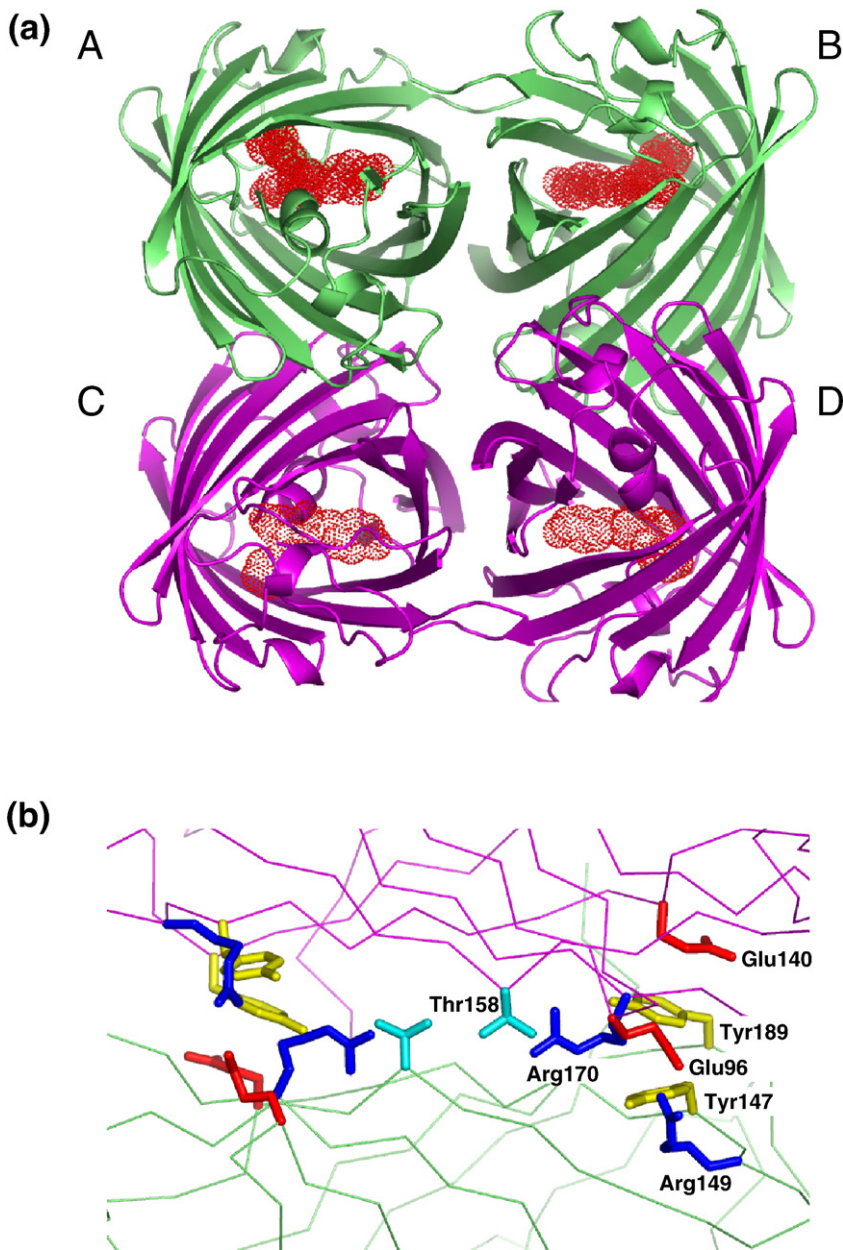


**Figure 1.** Crystal structure of Kaede. (a) Ribbon representation of the red form Kaede tetramer, with the central chromophore shown as red dot. The dimer observed in an asymmetric unit is shown in the same color (A–B and C–D pairs). (b) The dimer interface between A and B (or C and D). Each monomer is shown as C $\alpha$  traces in magenta or green. The side-chains of the amino acids responsible for dimer formation are shown as sticks. Thr158 is depicted in cyan, Arg149 and Arg170 in blue, Glu96 and Glu140 in red, Tyr147 and Tyr189 in yellow. Figures were generated using PyMOL [<http://www.pymol.org>].

sessing an 11-stranded  $\beta$ -barrel ( $\beta$ -can) with a central  $\alpha$ -helix. A chromophore, the post-translational modification of His62-Tyr63-Gly64, is found

**Table 1.** Cross-table of structural similarity between Kaede, EosFP and DsRed

| rmsd (Å) (of a.a.)    |                                 |                                 |              |
|-----------------------|---------------------------------|---------------------------------|--------------|
| Sequence identity (%) | Kaede (PDB code 2GW3)           | EosFP (1ZUX)                    | DsRed (1G7K) |
| Kaede                 |                                 |                                 |              |
| EosFP                 | 0.78<br>(876 C $\alpha$ )<br>84 |                                 |              |
| DsRed                 | 1.57<br>(872 C $\alpha$ )<br>47 | 1.50<br>(872 C $\alpha$ )<br>49 |              |

a.a., amino acid(s).

inside the  $\beta$ -barrel structure linked to the central helix covalently.

The Kaede tetramer is generated via crystallographic symmetry. This oligomerization state is consistent with our previous biochemical data that Kaede is a tetrameric in solution.<sup>16</sup> The orientation of each protomer is almost identical to that of DsRed (r.m.s.d. of 1.57 Å for 872 C $\alpha$ ; Table 1) and EosFP, a homolog of Kaede (0.78 Å for 876 C $\alpha$ ); four molecules are packed tightly in one unit of a tetramer through two extensive protein interaction surfaces. As reported in the DsRed crystal structures, each protomer is arranged as a dimer of chain A and B, which appears in the asymmetric unit in Kaede structure. The dimer interface of these symmetrically related protomers involves a large number of interactions (Figure 1(b)). The most significant interaction is hydrogen bonding of the Thr158 side-chain between chain A and B. Thr158 is

conserved in both Kaede and EosFP (Supplementary Data, Figure 1). In DsRed, Thr158 is substituted to His (162 in DsRed), which forms a polar interaction with another Thr158 at the dimer interface. In EosFP, mutation of Thr158 to His breaks the tetramer formation,<sup>17</sup> indicating that Kaede and EosFP have different oligomerization interaction from DsRed.

We also observe many interactions involving salt bridges and polar residues. Side-chains of Arg149, Glu96, Tyr147, Tyr189, Arg170 and Glu140, all of which are responsible for the dimerization, are also conserved in DsRed. It is noteworthy that Campbell *et al.* were successful in the production of a monomeric DsRed by mutating 33 amino acids including

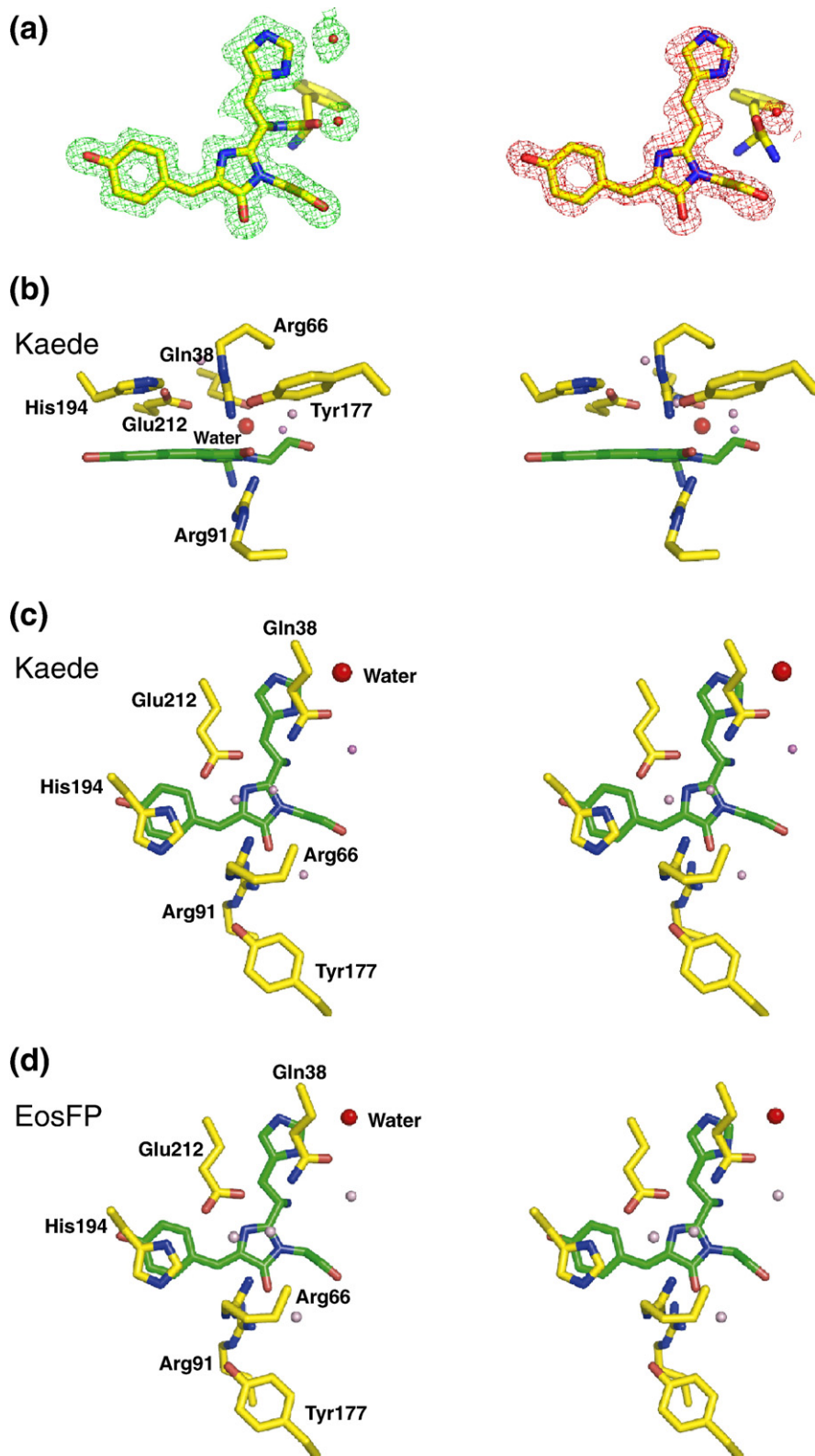


**Figure 2.** Photo-induced conformational changes in the chromophore vicinity. (a)  $F_o - F_c$  omit maps (occupancy of all chromophore and water atoms in the model discussed in the text set to zero) of the green and red chromophores (left and right, respectively). The maps are contoured at  $1.8\sigma$ . (b) and (c) Stereo view of the green-chromophore structure vicinity in Kaede. The orientation in (c) is related by a  $90^\circ$  rotation about a horizontal axis with (b). Carbon atoms in the chromophore are colored green, the rest of the carbon atoms in Gln38, Arg66, Arg91, Tyr177, His194 and Glu212 are in yellow. Nitrogen atoms are shown in blue, oxygen in red. The water molecule close to the His62 ring is shown by bigger red dots. Other water molecules involved in the proton network are shown in pink. (d) Stereo view of the green-chromophore structure vicinity in EosFP. The orientation is the same as (c) in Kaede.

these key residues to inhibit the dimer interactions.<sup>25</sup> The Kaede structure also contains the interactions of C-terminal tails indicated as “arm-in-arm” in DsRed structure to stabilize tetramer formation,<sup>26</sup> which faces to the solvent both in Kaede and DsRed structures.

The interaction between A and C (or B and D) is dominated by hydrophobic interactions. Although the A/C interface reveals a larger surface area than that of A/B (1030 Å<sup>2</sup> and 902 Å<sup>2</sup>, respectively), few hydrogen bonds are observed between A and C, except Glu90 carboxyl group bonding to the backbone carbonyl nitrogen atom of Asn124. This observation indicates that Kaede has a minimal unit consisting of a stable dimer, and forms a tetramer through the polar residues described above.

### Green and red chromophores and their environments

The chromophore of Kaede is formed by a similar autocatalytic mechanism with that of GFP or DsRed. The cyclization and dehydrogenation of tripeptide from residues His62, Tyr63 and Gly64, give rise to 2-[(1E)-2-(4-imidazolyl)ethenyl]-4-(*p*-hydroxybenzylidene)-5-imidazolinone, whose imidazole, benzylidene, and imidazolinone rings are observed to be coplanar. As reported in our previous study, the formal  $\beta$ -elimination reaction is accomplished by UV irradiation, resulting in peptide cleavage between the N $^{\alpha}$  and the C $^{\alpha}$  of His62.<sup>18</sup> In the electron density map, the peptide cleavage site and the resulting chromophore are clearly recognizable, and the density distribution of the chromophore region is surprisingly similar between the green and red forms (Figure 2(a)), with the exception of the cleaved bond. The environments of the chromophore are almost identical to each other; both feature a

widespread  $\pi$ -system on the chromophore plane. The chromophore region contains another  $\pi$ -bonding system layer stacked beneath the chromophore moiety. This extends the conjugated  $\pi$ -system leading to delocalization of electrons in the photo-conversion reaction steps (Figure 2(b) and (c)). The imidazole ring of His194 is located beneath the chromophore  $\pi$ -plane to form non-polar interactions. The side-chains of Gln38 and Glu212 are also in the close proximity to the chromophore, stabilized by hydrogen bonding interactions with the imidazole ring of His194 and the amino group of Arg66 through water molecules (Figure 3). As such, the Kaede chromophore is buried in the  $\beta$ -can hydrophobic interior, forming an extensive network of hydrogen bonding and hydrophobic interactions (Figure 3). These observations are similar to those for EosFP, which also exhibits photo-induced protein cleavage and green-to-red conversion.<sup>24</sup> In both Kaede and EosFP, a major difference between the green and red form is the presence of a water molecule near the imidazole ring of His62, which is observed only in the green form (Figure 2(b) and (c)); this water molecule is located within an interaction distance to the imidazole ring of His62 (Figure 3) and forms a hydrogen bond with the side-chain oxygen atom of Gln38. Another water molecule forms hydrogen bonds with this oxygen of Gln38 and the backbone oxygen of Phe61 to stabilize their conformation. The temperature factors (*B*-factors) of these water molecules are 20.0 Å<sup>2</sup> and 14.6 Å<sup>2</sup>, respectively, indicating that they are well-ordered and thus stabilize the delocalization of the electrons (14.4 Å<sup>2</sup> for the overall average *B*-factor of the green form). The same water molecule was also observed in the green form of EosFP (Figure 2(d)) but was not included in the proposed mechanism of photoconversion.<sup>24</sup>

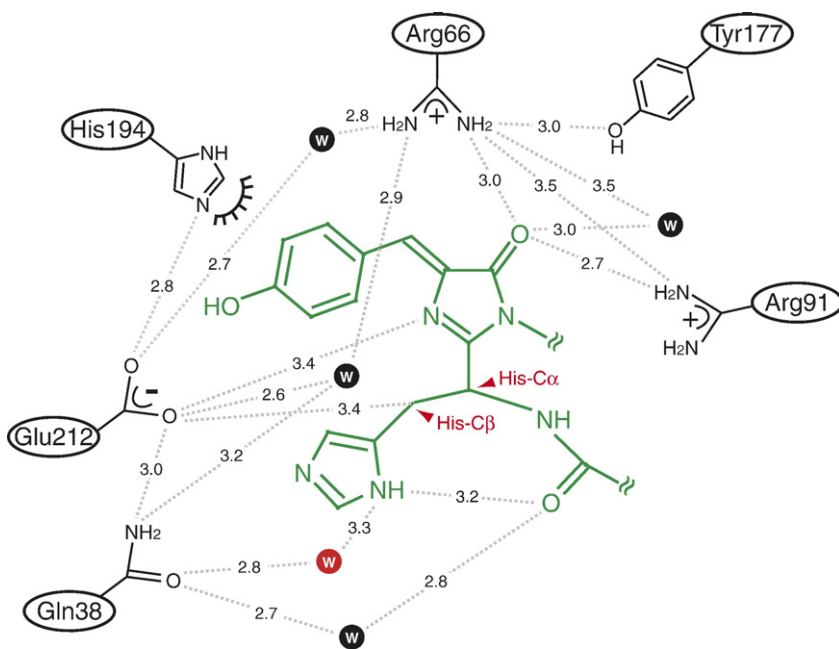


**Figure 3.** Scheme showing the interaction between the green chromophore and other residues in Kaede. The number indicates distance between atoms connected by the broken line below 3.5 Å. Water molecules are indicated by w. The van der Waals contact is indicated by an arc. The water molecule discussed in the text is colored red.

### Possible interpretation of photo-induced reaction mechanism

A possible mechanism of the red-chromophore formation in Kaede is shown in Figure 4. We propose that the peptide bond-cleavage reaction occurs first by the trigger of UV irradiation (Figure 4(c)–(d)) followed by the red-chromophore formation by the isomerization to generate  $\pi$ -conjugation between the green-chromophore and the imidazole (Figure 4(d)–(e)).

Excitation of the green form by UV light induces the formation of an activated *p*-quinone methide conjugated to oxyanion (Figure 4(a)–(b)).<sup>27</sup> Based on the typical  $pK_a$  value ( $\sim 7$ ) of imidazolium,<sup>28</sup> His62 imidazole should be present as a protonated form or neutral form. The positively charged imidazole should act as an acid catalyst for the cleavage reaction through the protonation to the carbonyl group of Phe61. The presence of water molecules near His62 should act favorably for the

protonated imidazole as well as for the protonated state of the amide carbonyl of Phe61. Movement of the lone electron pair at the oxygen atom in the imidazolinone ring results the cleavage of the peptide bond at His62 (Figure 4(c)–(d)).<sup>18</sup> In the crystal structure of the green form, the imidazole ring of His62 exists on the same plane as the  $\pi$ -conjugated green-chromophore moiety. The angle between the imidazolinone-C,  $C^\alpha$ ,  $N^\alpha$  of His62 is  $\sim 101^\circ$ ; this conformation is easily converted to form the transition state of the C–N bond cleavage reaction that requires particular stereo-electronic requirements.

The imidazole ring of His62 plays an essential role in the photo-induced cleavage reaction, since mutation of His62 to any other amino acid results in a failure in the photo-cleavage and photoconversion reaction.<sup>18</sup> Aromatic amino acids, such as phenylalanine and tyrosine, at position 62 do not appear to promote the cleavage reaction at ambient temperature. This result indicates that the positively

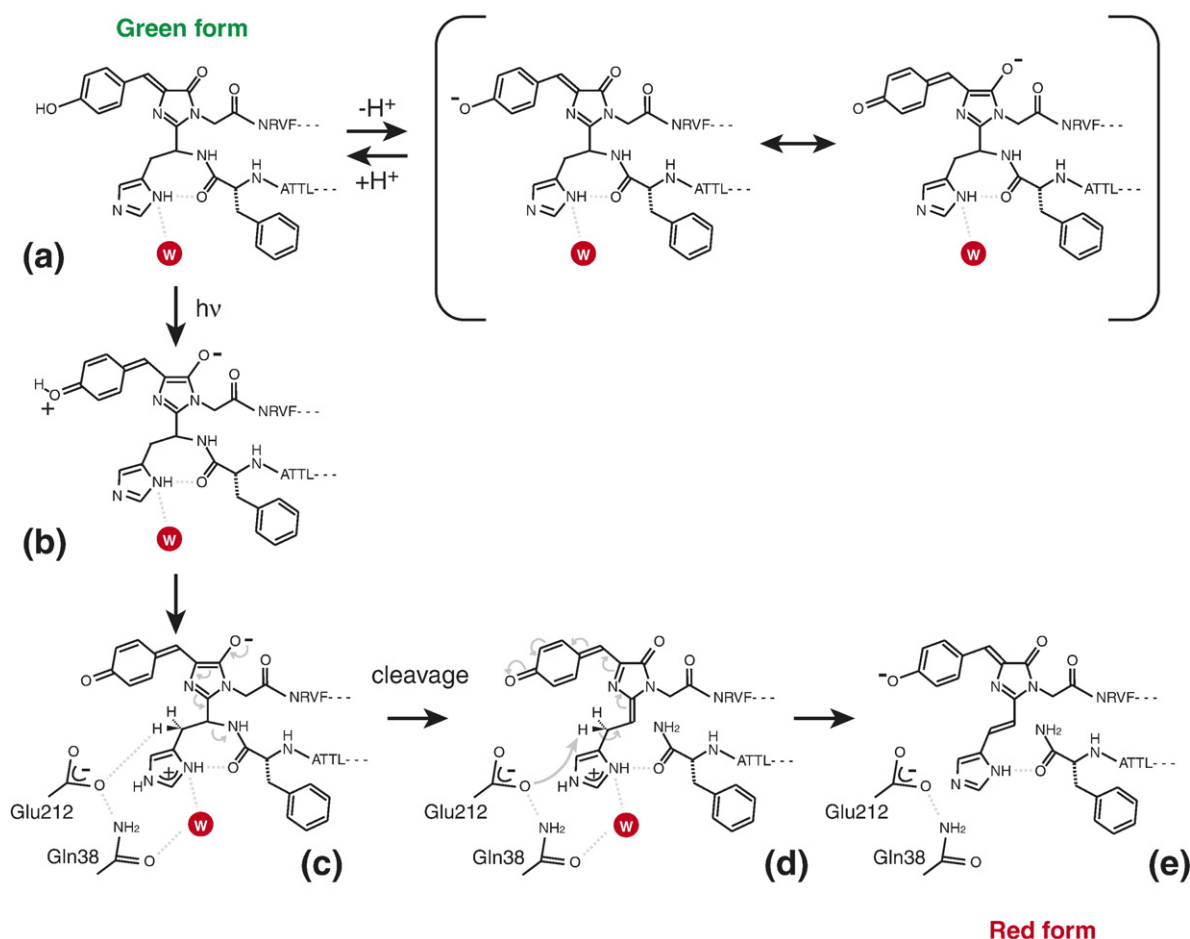


**Figure 4.** Proposed mechanism of the green-to-red photoconversion reaction. Scheme for the photo-induced chromophore extension and  $\beta$ -elimination reaction of Kaede. Chromophore derived from His62-Tyr63-Gly64 (4-(*p*-hydroxybenzylidene)-5-imidazolinone); (a) is excited by UV or violet light ( $h\nu$ ); (b) and releases a proton to form the excited intermediate (c). The water molecule stabilizing His62 imidazole ring protonation is indicated by a red circle. The  $\beta$ -elimination reaction occurs at  $N^\alpha$ – $C^\alpha$  of His62 to produce a carboxamide group-containing peptide. Glu212 acts as a base to abstract a proton from  $C^\beta$  of His62 (d), resulting in the widespread conjugated  $\pi$ -system by double bond formation between  $C^\alpha$  and  $C^\beta$  of His62 (e). The proton network including water molecules is shown in (c). Dotted lines indicate the interactions described in the text.

charged imidazole of the histidine is important in the cleavage reaction triggered by UV/vis irradiation. Moreover, leaving group ability of the carboxamide group at Phe61 has to be enhanced: Protonation of the carbonyl oxygen with the imidazolium proton of His62 is essential to proceed the cleavage reaction.

After the C–N bond cleavage reaction, Glu212, which is located within a reaction distance from His62, may act as a base for the abstraction of the C<sup>β</sup> proton and a double bond is isomerized to the position at C<sup>α</sup> and C<sup>β</sup> of His62 (Figure 4(e)). The positively charged imidazole of His62 and the double bond next to the C<sup>β</sup> position of His62 generated by the C–N cleavage should contribute to increasing the acidity of the C<sup>β</sup> proton of His62. As a consequence, Glu212 can easily abstract this C<sup>β</sup> proton. In the green form, there is no neighboring double bond to the C<sup>β</sup> of His62 and the abstraction of a proton at this position is energetically unfavorable. This reaction route *via* 4C and 4D was previously suggested from our biophysical analysis.<sup>18</sup>

Substitution of Glu212 to Gln results in the loss of the ability to proceed the photoconversion including the C–N cleavage reaction (data not shown). This observation indicates that the carboxylate also contributes to the cleavage step as well as the double bond isomerization step. In the Kaede green form, the side-chain of Glu212 forms a hydrogen bond with N<sup>ε</sup> of Gln38, which is stabilized by the hydrogen-bonding network of two water molecules near the His62 imidazole ring (Figure 3). This network should also stabilize the charged transition state of the C–N bond cleavage reaction. Therefore, UV/vis irradiation, His62, and Glu212 are all essential for the cleavage of the backbone and for the formation of the red-chromophore.

Conjugation of the imidazole ring to the green chromophore moiety results in generation of the long  $\pi$ -conjugation system that is responsible for generation of the red color. The crystal structure of the red form of Kaede does not have any water molecule near His62. The conjugation should render the pK<sub>a</sub> value of the imidazole ring lower than that in the green form. As a result, the imidazole of the red-chromophore is present as a neutral form, releasing the water molecule from its neighbor.

The crystal structures of EosFP in both green and red forms are markedly similar to those of Kaede (Figure 2(c) and (d)).<sup>24</sup> The tertiary arrangement of the interior chromophore is nearly identical between the two proteins. Moreover, a water molecule was found in the same position proximal to His62 in both EosFP and Kaede, but only in the green form. Based on the crystal structures of EosFP, Nienhaus *et al.* proposed an E2 mechanism for the photoconversion of EosFP: Glu212 acts as a base for the abstraction of the C<sup>β</sup> proton of His62 which triggers the C–N bond cleavage in a concerted manner.<sup>24</sup> As the authors indicated in their paper, this model is not consistent with the fact that the conversion accompanies photo-excitation with UV light. In addition, the

proposed E2 mechanism did not account for the role of the His62 proximal water molecule found in the green form of EosFP. These facts prompted us to reconsider the photoconversion mechanism of Kaede, and our model accounts for the role of the water molecule and the initiation of UV irradiation.

We believe that the C<sup>β</sup> proton will not be abstracted by a carboxylic acid, unless double-bond formation occurs next to the C<sup>β</sup> position of His62 in Kaede (Figure 4(d)). Although it is likely that His62 is positively charged by protonation, the level of the acidity of the C<sup>β</sup> proton of histidine is insufficient for the abstraction of the proton by carboxylate.<sup>29</sup> Instead, we propose that UV irradiation triggers the C–N cleavage reaction, leading to formation of a double bond at the neighboring position to the C<sup>β</sup> proton of His62. This double bond formation causes an increase of C<sup>β</sup> proton acidity (Figure 4(c)), which enables Glu212 to abstract the C<sup>β</sup> proton and the red-chromophore forms. In our proposed mechanism, Glu212 participates in the C–N bond cleavage step by stabilizing the cleavage transition state by forming the hydrogen bond network with Gln38, His62 and Phe61 *via* water molecules rather than by direct abstraction of the C<sup>β</sup> proton to trigger the cleavage (Figure 4(c)). After the C–N bond cleavage, Glu212 promotes the isomerization of the double bond as a base. Interestingly, the conformation of the chromophore surrounding

**Table 2.** Summary of crystallographic analysis and refinement statistics

|   | Kaede green-form                                       | Kaede red-form   |
|---|--|--|
| <i>Data collection</i>  |  |  |
| Space group   | C2   | C2   |
| Unit cell dimensions (Å)  | <i>a</i> = 132.5<br><i>b</i> = 80.5<br><i>c</i> = 53.5 | <i>a</i> = 132.2<br><i>b</i> = 81.2<br><i>c</i> = 53.5 |
| (deg.)  | $\beta$ = 113.8  | $\beta$ = 113.9  |
| X-ray source  | APS 19BM   | SPring-8<br>BL44XU                                     |
| Wavelength (Å)  | 0.9795   | 0.9000   |
| Data range (Å)  | 50–1.4   | 25–1.6   |
| Unique reflections  | 99,275   | 67,774   |
| Completeness (%) <sup>a</sup>   | 99.7 (99.5)  | 99.5 (99.5)  |
| <i>I</i> / $\sigma$ ( <i>I</i> ) <sup>a</sup>                         | 28.0 (3.9)   | 24.9 (6.0)   |
| <i>R</i> <sub>merge</sub> <sup>a,b</sup>                              | 0.061 (0.398)  | 0.084 (0.233)  |
| <i>Refinement</i>   |  |  |
| Resolution range (Å)  | 25–1.4   | 25–1.6   |
| No. of reflections in working set                                     | 83,826   | 60,921   |
| <i>R</i> <sub>cryst</sub> ( <i>R</i> <sub>free</sub> ) <sup>a,c</sup> | 19.7 (21.4)  | 19.8 (21.3)  |
| rmsd bond length (Å)  | 0.007  | 0.006  |
| rmsd bond angles (°)  | 1.58   | 1.51   |
| No. of protein atoms  | 3554   | 3554   |
| No. of ions   | 4  | 4  |
| No. of solvent atoms  | 402  | 437  |

<sup>a</sup> Numbers in parentheses refer to statistics for the highest shell of data.

<sup>b</sup>  $R_{\text{merge}} = \sum |I_{\text{obs}} - \langle I \rangle| / \sum I_{\text{obs}}$ , where  $I_{\text{obs}}$  is the intensity measurement and  $\langle I \rangle$  is the mean intensity for multiply recorded reflections (30).

<sup>c</sup>  $R_{\text{cryst}}$  and  $R_{\text{free}} = \sum ||F_{\text{obs}}| - |F_{\text{calc}}|| / |F_{\text{obs}}|$  for reflections in the working and test sets, respectively. The *R*-free value was calculated using a randomly selected 10% of the data set that was omitted through all stages of refinement.

residues is nearly identical between the green and red forms, indicating that Kaede accomplish the photoconversion reaction efficiently with little activation energy barrier. This is also the case for EosFP.<sup>24</sup>

In summary, we have analyzed crystal structures of Kaede in the green and red forms. We propose that the mechanism of the C–N bond cleavage reaction is first initiated by UV irradiation, which is followed by the double-bond isomerization in the photoconversion of Kaede. This mechanism is different from that proposed for EosFP. Further experiments are needed to address whether Kaede and EosFP use different photoconversion mechanisms and more specifically how proton transfer reactions take place in each protein.

## Materials and Methods

### Protein purification and crystallization

The green-form of recombinant Kaede was produced in *Escherichia coli* and purified as described.<sup>16</sup> The protein was concentrated to 15 mg/ml in buffer containing 10 mM Tris–HCl (pH 8.0), 100 mM NaCl and 1 mM DTT.

Crystals of the green form were grown at 20 °C in the dark by vapor diffusion with drops containing 1 µl of protein solution and 1 µl of reservoir solution containing 0.1 M Tris–HCl (pH 8.0), 2 M Li<sub>2</sub>SO<sub>4</sub>, and 2 mM NiCl<sub>2</sub>. Crystals of the red form were obtained by irradiation of green form crystals in the reservoir solution to the sunlight for three days. For data collection, crystals were transferred into a cryo-protectant solution containing the reservoir solution supplemented with 27% (v/v) glycerol and flash frozen in liquid nitrogen.

### Crystallography

The data set for the green form was collected at the Advanced Photon Source (Argonne, IL) on beamline 19-BM. Data processing and reduction were carried out with the HKL2000 program suite,<sup>30</sup> and for the red-form at Spring-8 on beamline 44-XU processed with MOSFLM<sup>31</sup> and programs of the CCP4 suite.<sup>32</sup> Both crystals belong to space group C2 (for the green-form with cell dimensions  $a = 132.5$  Å,  $b = 80.5$  Å,  $c = 53.5$  Å,  $\beta = 113.8^\circ$  and for the red-form with  $a = 132.2$  Å,  $b = 81.2$  Å,  $c = 53.5$  Å,  $\beta = 113.9^\circ$ ) and their asymmetric unit contains two molecules and a solvent content of 51%.

The structure of green-form Kaede was solved by molecular replacement with the program CNS<sup>33</sup> using the coordinates of the single polypeptide chain in DsRed (PDB code 1G7K) as a search model. Manual rebuilding was performed with XtalView,<sup>34</sup> followed by iterative rounds of refinement using simulated annealing and positional refinement in CNS.<sup>33</sup> The initial electron density map of the red-form was calculated with FFT<sup>32</sup> using the green-form structure and refined with CNS, independently. Chromophores of both forms were modeled and refined in the final stages of refinement (Table 2).

### Protein Data Bank accession codes

The atomic coordinates and structure factors (codes 2GW3 and 2GW4 for the green and red forms, respectively) have been deposited in the RCSB Protein Data Bank.

## Acknowledgements

We thank Dr Atsushi Nakagawa and Jane Gooding for critical reading of the manuscript, and the staff of the Advanced Photon Source and SPring-8 for assistance with the data collection. I.H. acknowledges the Canadian Institutes of Health Research (CIHR) for a postdoctoral fellowship. M.I. holds a Canada Research Chair in Cancer Structural Biology. This work was supported by a grant from CIHR.

## Supplementary Data

Supplementary data associated with this article can be found, in the online version, at [doi:10.1016/j.jmb.2007.06.037](https://doi.org/10.1016/j.jmb.2007.06.037)

## References

1. Tsien, R. Y. & Prasher, D. C. (1998). *Molecular Biology and Mutation of Green Fluorescent Protein*, Wiley-Liss, New York.
2. Ormö, M., Cubitt, A. B., Kallio, K., Gross, L. A., Tsien, R. Y. & Remington, S. J. (1996). Crystal structure of the *Aequorea victoria* green fluorescent protein. *Science*, **273**, 1392–1395.
3. Heim, R., Prasher, D. C. & Tsien, R. Y. (1994). Wavelength mutations and posttranslational autooxidation of green fluorescent protein. *Proc. Natl Acad. Sci. USA*, **91**, 12501–12504.
4. Remington, S. J. (2000). Structural basis for understanding spectral variations in green fluorescent protein. *Methods. Enzymol.* **305**, 196–211.
5. Heim, R. & Tsien, R. Y. (1996). Engineering green fluorescent protein for improved brightness, longer wavelengths and fluorescence resonance energy transfer. *Curr. Biol.* **6**, 178–182.
6. Wachter, R. M., Elsliger, M. A., Kallio, K., Hanson, G. T. & Remington, S. J. (1996). Structural basis of spectral shifts in the yellow-emission variants of green fluorescent protein. *Structure*, **6**, 1267–1277.
7. Tsien, R. Y. (2003). Imagining imaging's future. *Nature Rev. Mol. Cell. Biol.* **00**, SS16–SS21.
8. Miyawaki, A., Sawano, A. & Kogure, T. (2003). Lighting up cells: labelling proteins with fluorophores. *Nature Cell. Biol.* **00**, S1–S7.
9. Cubitt, A. B., Woollenweber, L. A. & Heim, R. (1999). Understanding structure-function relationships in the *Aequorea victoria* green fluorescent protein. *Methods Cell Biol.* **58**, 19–30.
10. Mitra, R. D., Silva, C. M. & Youvan, D. C. (1996). Fluorescence resonance energy transfer between blue-emitting and red-shifted excitation derivatives of the green fluorescent protein. *Gene*, **173**, 13–17.
11. Mizuno, H., Sawano, A., Eli, P., Hama, H. & Miyawaki, A. (2001). Red fluorescent protein from *Discosoma* as a



- fusion tag and a partner for fluorescence resonance energy transfer. *Biochemistry*, **40**, 2502–2510.
12. Marchant, J. S., Stutzmann, G. E., Leissring, M. A., LaFerla, F. M. & Parker, I. (2001). Multiphoton-evoked color change of DsRed as an optical highlighter for cellular and subcellular labeling. *Nature Biotechnol.* **19**, 645–649.
  13. Wilmann, P. G., Petersen, J., Pettikiriachchi, A., Buckle, A. M., Smith, S. C., Olsen, S. *et al.* (2005). The 2.1 Å crystal structure of the far-red fluorescent protein HcRed: inherent conformational flexibility of the chromophore. *J. Mol. Biol.* **349**, 223–237.
  14. Wiedenmann, J., Schenk, A., Röcker, C., Girod, A., Spindler, K. D. & Nienhaus, G. U. (2002). A far-red fluorescent protein with fast maturation and reduced oligomerization tendency from *Entacmaea quadricolor* (Anthozoa, Actinaria). *Proc. Natl Acad. Sci. USA*, **99**, 11646–11651.
  15. Petersen, J., Wilmann, P. G., Beddoe, T., Oakley, A. J., Devenish, R. J., Prescott, M. & Rossjohn, J. (2003). The 2.0-Å crystal structure of eqFP611, a far red fluorescent protein from the sea anemone *Entacmaea quadricolor*. *J. Biol. Chem.* **278**, 44626–44631.
  16. Ando, R., Hama, H., Yamamoto-Hino, M., Mizuno, H. & Miyawaki, A. (2002). An optical marker based on the UV-induced green-to-red photoconversion of a fluorescent protein. *Proc. Natl Acad. Sci. USA*, **99**, 12651–12656.
  17. Wiedenmann, J., Ivanchenko, S., Oswald, F., Schmitt, F., Röcker, C., Salih, A. *et al.* (2004). EosFP, a fluorescent marker protein with UV-inducible green-to-red fluorescence conversion. *Proc. Natl Acad. Sci. USA*, **101**, 15905–15910.
  18. Mizuno, H., Mal, T. K., Tong, K. I., Ando, R., Furuta, T., Ikura, M. & Miyawaki, A. (2003). Photo-induced peptide cleavage in the green-to-red conversion of a fluorescent protein. *Mol. Cell*, **12**, 1051–1058.
  19. Gross, L. A., Baird, G. S., Hoffman, R. C., Baldridge, K. K. & Tsien, R. Y. (2000). The structure of the chromophore within DsRed, a red fluorescent protein from coral. *Proc. Natl Acad. Sci. USA*, **97**, 11990–11995.
  20. Martynov, V. I., Maksimov, B. I., Martynova, N. Y., Pakhomov, A. A., Gurskaya, N. G. & Lukyanov, S. A. (2003). A purple-blue chromoprotein from *Goniopora tenuidens* belongs to the DsRed subfamily of GFP-like proteins. *J. Biol. Chem.* **278**, 46288–46292.
  21. Zagranichny, V. E., Rudenko, N. V., Gorokhovatsky, A. Y., Zakharov, M. V., Shenkarev, Z. O., Balashova, T. A. & Arseniev, A. S. (2004). zFP538, a yellow fluorescent protein from coral, belongs to the DsRed subfamily of GFP-like proteins but possesses the unexpected site of fragmentation. *Biochemistry*, **43**, 4764–4772.
  22. Remington, S. J., Wachter, R. M., Yarbrough, D. K., Branchaud, B., Anderson, D. C., Kallio, K. & Lukyanov, K. A. (2005). zFP538, a yellow-fluorescent protein from *Zoanthus*, contains a novel three-ring chromophore. *Biochemistry*, **44**, 202–212.
  23. Quillin, M. L., Anstrom, D. M., Shu, X., O'Leary, S., Kallio, K., Chudakov, D. M. & Remington, S. J. (2005). Kindling fluorescent protein from *Anemonia sulcata*: dark-state structure at 1.38 Å resolution. *Biochemistry*, **44**, 5774–5787.
  24. Nienhaus, K., Nienhaus, G. U., Wiedenmann, J. & Nar, H. (2005). Structural basis for photo-induced protein cleavage and green-to-red conversion of fluorescent protein EosFP. *Proc. Natl Acad. Sci. USA*, **102**, 9156–9159.
  25. Campbell, R. E., Tour, O., Palmer, A. E., Steinbach, P. A., Baird, G. S., Zacharias, D. A. & Tsien, R. Y. (2002). A monomeric red fluorescent protein. *Proc. Natl Acad. Sci. USA*, **99**, 7877–7882.
  26. Wall, M. A., Socolich, M. & Ranganathan, R. (2000). The structural basis for red fluorescence in the tetrameric GFP homolog DsRed. *Nature Struct. Biol.* **7**, 1133–1138.
  27. Tozzini, V. & Nifosi, R. (2001). Ab initio molecular dynamics of the green fluorescent protein (GFP) chromophore: an insight into the photoinduced dynamics of green fluorescent proteins. *J. Phys. Chem. ser. B*, **105**, 5797–5803.
  28. Sayer, J. M., Peskin, M. & Jencks, W. P. (1973). Imine-forming elimination reactions. I. General base acid catalysis and influence of the nitrogen substituent on rates and equilibria for carbinolamine dehydration. *J. Am. Chem. Soc.* **95**, 4277–4287.
  29. Fu, Y., Liu, L., Li, R. Q. & Guo, Q. X. (2004). First-principle predictions of absolute pK<sub>a</sub>'s of organic acids in dimethyl sulfoxide solution. *J. Am. Chem. Soc.* **126**, 814–822.
  30. Otwinowski, Z. & Minor, W. (1997). Processing of X-ray diffraction data collected in oscillation mode. *Methods Enzymol.* **276**, 307–326.
  31. Leslie, A. G. W. (1992). CCP4 and ESF-EACMB Newsletter on Protein Crystallography, **26**.
  32. Collaborative Computational Project, Number 4 (1994). The CCP4 suite: programs for protein crystallography. *Acta Crystallog. sect. D*, **50**, 760–763.
  33. Brunger, A. T., Adams, P. D., Clore, G. M., DeLano, W. L., Gros, P., Grosse-Kunstleve, R. W. *et al.* (1998). Crystallography and NMR system: a new software suite for macromolecular structure determination. *Acta Crystallog. sect. D*, **54**, 905–921.
  34. McRee, D. E. (1999). XtalView/Xfit—A versatile program for manipulating atomic coordinates and electron density. *J. Struct. Biol.* **125**, 156–165.

Edited by R. Huber

(Received 16 March 2007; received in revised form 8 June 2007; accepted 13 June 2007)  
Available online 19 June 2007